

Optimized Basis Sets for Calculation of Electron Paramagnetic Resonance Hyperfine Coupling Constants: aug-cc-pVTZ-J for the 3d Atoms Sc–Zn

Erik Donovan Hedegård,[†] Jacob Kongsted,[†] and Stephan P. A. Sauer^{*,‡}

[†]Department of Chemistry and Physics, University of Southern Denmark, Odense, Denmark

[‡]Department of Chemistry, University of Copenhagen, Copenhagen, Denmark

 Supporting Information

ABSTRACT: The hyperfine coupling tensor of electron paramagnetic resonance (EPR), describing the interaction between an electron and a given nuclei, depends strongly on the electron density at the nucleus. With standard Gaussian-type orbital basis sets (GTOs), employed in most calculations, it is difficult to obtain converged results of the hyperfine coupling tensor, and basis sets with more flexible core regions have therefore been devised. To this class of core property basis sets belong the aug-cc-pVTZ-J basis sets developed for the s- and p-block atoms. Here, we extend the aug-cc-pVTZ-J basis sets to include the 3d elements Sc–Zn. The converged optimal basis sets are throughout the series described by a (25s17p10d3f2g)/[17s10p7d3f2g] contraction scheme, where four tight s-, one tight p-, and one tight d-type function have been added to the original aug-cc-pVTZ basis sets. The basis sets are generally contracted, and molecular orbital coefficients are used as contraction coefficients. By validation studies with different functionals and compounds, it is shown that the values of the contraction coefficient are effectively independent of the compound used in their generation and the exchange-correlation functional employed in the calculation.

INTRODUCTION

Electron paramagnetic resonance (EPR) has, since its early development in the 1940s,¹ evolved to be a spectroscopic method of fundamental importance with applications in a wide range of chemical fields, including d-block metals,² organic radicals,^{3–5} and biomimetic chemistry.^{6–8} The experimental spectra are usually interpreted by the introduction of an effective spin Hamiltonian where the physical quantities enter as fitting parameters. Within d-block metal chemistry, the effective spin Hamiltonian was developed with impressing insight by Abragam and Pryce, using a framework of crystal field theory^{9–13}

$$\hat{\mathcal{H}}_{\text{eff}} = \mu_B \hat{\mathbf{S}} \mathbf{g} \mathbf{B} + \sum_{\alpha} \hat{\mathbf{S}} \mathbf{A}_{\alpha} \hat{\mathbf{I}}_{\alpha} + D \left[\hat{S}_z^2 - \frac{1}{3} S(S+1) \right] + E [\hat{S}_x^2 - \hat{S}_y^2] \quad (1)$$

Here, $\hat{\mathbf{S}}$ is the total spin of the molecule and \mathbf{B} is the external magnetic field. The \mathbf{g} tensor is a 3×3 tensor, describing the interaction of the external field with the spin of the unpaired electron(s) in the molecule. D and E enter for $S > 1/2$ systems and are zero field splitting constants which depend on the exact symmetry of the paramagnetic center. The hyperfine coupling tensor, \mathbf{A} , is the target of the present study. As the \mathbf{g} tensor, the hyperfine coupling tensor is a 3×3 tensor. It describes the interaction between the unpaired electron(s) in the molecular system and the magnetic moments of the nuclei, $\hat{\mathbf{I}}_{\alpha}$. Accordingly, the sum in eq 1 runs over the nuclei in the molecule which have nonzero spin. The hyperfine coupling tensor is used as a sensitive probe for the immediate coordination environment of d-block metals, for instance in the studies of the cytochrome P450 enzymes^{14–17} or the active species in photosystem II.¹⁸

From textbooks on the magnetic theory of quantum mechanics^{1,19} it is known that \mathbf{A} , to first order, is composed of an isotropic (Fermi-contact) term and a contribution due to anisotropic spin-dipolar interactions

$$\mathbf{A}_{\text{tot}} = \mathbf{A}_{\text{iso}} + \mathbf{A}_{\text{SD}} \quad (2)$$

The components of the isotropic, \mathbf{A}_{iso} , and anisotropic, \mathbf{A}_{SD} , spin dipolar hyperfine coupling tensors can be calculated from first principles from the N -electron, molecular Born–Oppenheimer wave function, Ψ , as

$$A_{\text{iso}, \alpha\beta} = \frac{\hbar \mu_0}{3m_e} \frac{eg_K g_K \mu_N}{\langle \Psi | \hat{S}_{\alpha} | \Psi \rangle} \langle \Psi | \sum_i \delta(\mathbf{r}_i - \mathbf{R}_K) \hat{s}_{i,\beta} | \Psi \rangle \quad (3)$$

$$A_{\text{SD}, \alpha\beta} = \frac{\hbar \mu_0}{8\pi m_e} \frac{eg_K g_K \mu_N}{\langle \Psi | \hat{S}_{\alpha} | \Psi \rangle} \langle \Psi | \sum_i \frac{3(\hat{s}_i(\mathbf{r}_i - \mathbf{R}_K))(r_{\beta} - R_{K,\beta})}{|\mathbf{r}_i - \mathbf{R}_K|^5} - \frac{\hat{s}_{i,\beta}}{|\mathbf{r}_i - \mathbf{R}_K|^3} | \Psi \rangle \quad (4)$$

where α and β are Cartesian components and the physical constants have their usual meaning.¹⁹ \mathbf{r}_i and \mathbf{R}_K are coordinates for the i th electron and the K th nucleus, respectively, and $\delta(\mathbf{r}_i - \mathbf{R}_K)$ denotes the Dirac δ function in which the expectation value over Ψ returns the electron density at nucleus K . Here, the Dirac δ function is multiplied with the spin operator for the i th electron, $\hat{s}_{i,\beta}$, thus returning the spin density at the K th nucleus. A representation which leads to a diagonal total tensor, \mathbf{A}_{tot} is usually chosen, and this practice is followed in this work. However, *a priori* the

Received: August 21, 2011

Published: November 14, 2011

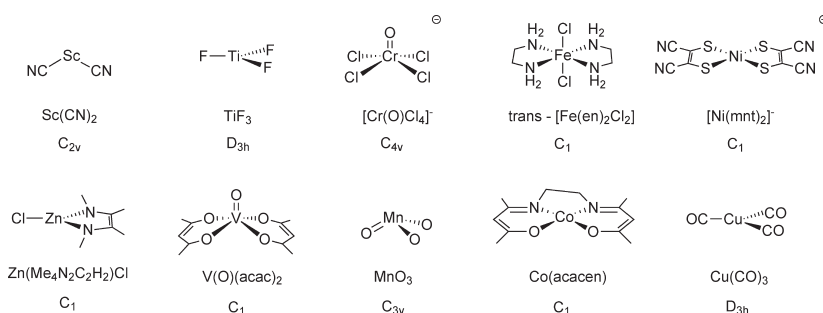


Figure 1. Training set 1 used for construction of the aug-cc-pVTZ-Juc basis set.

tensors are not represented by diagonal matrices. Further contributions arise if spin–orbit coupling is considered,²⁰ but such an effect will be left out in this study.

Calculation of A_{tot} from first principles has unfortunately proven to be a difficult task, and early attempts were met with little success.¹³ Early studies by Watson and Freeman²¹ concluded that the core level spin-polarization was crucial for the correct description of hyperfine couplings. A wide range of studies on small systems in recent decades^{22–33} have shown that highly correlated methods and basis sets with a flexible core region must be invoked to recover this core-level spin polarization. The special basis set requirements arise due to the Dirac δ function in the expression for A_{iso} , which usually is much larger than that for A_{SD} . Accordingly, the basis set should provide an accurate description of the core (and semicore) spin polarization effects.³⁴ It is by now well-recognized that standard Gaussian basis sets are in general not able to model properties which depend on the core electron density at sufficient accuracy. The problem is that such basis sets are optimized to describe the valence region and do not fulfill the correct nuclear cusp condition leading to slow convergence with increasing basis set size. The combination of slow convergence both with respect to the level of sophistication in theory and basis sets size leads to severe restrictions in the complexity of the studied systems. For systems with d-block metals, only small (often linear) systems have been treated comprehensively^{35,36} and with *ad hoc* devised basis sets. With the introduction of density functional theory, large parts of the dynamic electron correlation can be handled at much reduced cost, and calculation of hyperfine coupling tensors for d-block metal complexes is now tractable. Results from the p-block elements using DFT for hyperfine coupling constants have generally been promising,^{37–40} and several benchmark studies for d-block metal compounds have already emerged.^{36,41,42} Nevertheless, these benchmark studies focus mainly on the exchange-correlation functional, while the first-principle calculation of hyperfine coupling constants can be done at reduced cost and much more consistently if flexible, yet efficient basis sets were devised for the d-block metals. Several authors have shown that it is possible to modify Gaussian basis sets to describe core properties,^{23,34,43–49} but this has mostly focused on s- and p-block elements and few choices are available for the d-block.⁵⁰

In this paper, we extend the core-property basis aug-cc-pVTZ-J^{51–57} to the 3d metals Sc–Zn, such that accurate hyperfine couplings can be obtained for both metal and ligand spheres, using the same type of basis sets. This has not yet been possible within theoretical/computational d-block chemistry. It should be emphasized that the aug-cc-pVTZ-J basis sets for s- and p-block elements originally were optimized to describe nuclear magnetic

resonance spin–spin couplings. However, the d-block metals often contain unpaired electrons, usually situated in orbitals of high d character and have therefore traditionally been investigated by EPR. Seeing that the basis set requirements are similar in the description of NMR and EPR hyperfine couplings, we have here chosen an EPR framework, despite it meaning we have to deal with open-shell systems, which traditionally have been much more difficult to handle in terms of convergence and computer time.

METHODS

All calculations of hyperfine coupling constants were performed with the ORCA program⁵⁸ at the DFT level of theory. Throughout all calculations, the integration grid was always kept very large (IntAcc = 6 and AngularGrid = 7) to ensure that the core density was correctly described. Several studies on both main group^{59–61} and d-block metal complexes^{36,41,42} with a variety of different functionals have proven that A_{tot} can be quite sensitive to the exchange-correlation functional. Accordingly, we have used a small selection of functionals. For the calculation of hyperfine couplings, two GGA functionals, BP86^{62,63} and PBE,⁶⁴ a meta-GGA functional, TPSS,⁶⁵ and one hybrid-meta GGA functional, TPSSH,⁶⁵ were employed.

Basis Set Construction. The modification of the original aug-cc-pVTZ^{66–69} basis sets is performed for a set of molecules with atoms from the first row d-block metals (Figure 1, described in detail in the following subsection). This set is henceforth referred to as “training set 1”. Using this training set, the original basis sets are gradually decontracted. After decontraction, we add tight functions in an even-tempered manner as described in earlier work,^{51–57} starting with s-type functions. From the fully decontracted basis set, augmented with a sufficient number of tight s-type functions, we create two series where the first has tight p-type functions and the second, tight d-type functions. The tight p- and d-type functions which have a non-negligible effect on the hyperfine coupling tensor are included in the final basis sets. The uncontracted primitives and additional tight functions are recontracted using the molecular orbital coefficients of metal s-, p-, and d-character for the molecules in training set 1. To avoid bias in the final basis sets, the MO coefficients are compared to MO coefficients from a second set of molecules, henceforth denoted “training set 2” (Figure 2). Care has been taken to include metal complexes with very distinct ligand environments in the two training sets. To compare the MO coefficients from orbitals in the reference compounds (compounds in training set 1) and the corresponding metal complex in training set 2, the MOs must be renormalized. This is necessary as the orbitals with metal character also might contain some “contamination” of ligand orbitals, which will differ between training sets 1 and 2. Using the orbital of 1s character in TiF_3 as an

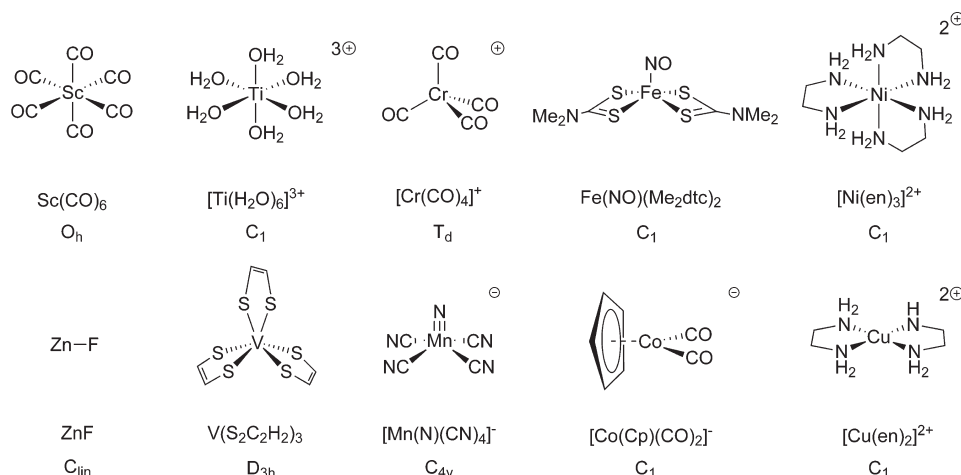


Figure 2. Training set 2 used under recontraction of the aug-cc-pVTZ-Juc to the aug-cc-pVTZ-J basis set.

example, the renormalization is done by using the ratio between the largest MO coefficient within the *s* primitive functions, comprising the 1s metal orbital and the corresponding metal *s* primitive MO coefficient in training set 2. All MO coefficients for *s*-type primitives within the orbital of metal 1s character in the reference compound are multiplied by this ratio. This method is repeated for orbitals of 2s and 3s, 2p and 3p, and 3d character. The renormalized coefficients are shown in Figures 9, 10, and 11. Despite this procedure being necessary to allow for a strict comparison, it has in fact little practical implication, as the original *s*-, *p*-, and *d*-type function coefficients and the renormalized coefficients are very close to each other.

For the 2p and 3p orbitals, one must choose between three orbitals, p_x , p_y , or p_z . A similar problem occurs in the contraction of the five *d* orbitals. Generally, the orbital with the largest *p* or *d* character is chosen, deemed from the MO coefficient sum of squares. For the *p* orbitals, this makes little difference, as the sum of squares are similar for all three orbitals and in all cases the p_z orbital is chosen. For the *d* orbitals, there is some difference in the sum of squares, and these have been investigated in detail.

Molecular Training Sets. The molecular geometries used are equilibrium geometries, optimized using the Gaussian program⁷⁰ with the BP86 functional and a TZVP basis set from the Ahlrichs group.^{71,72} For all molecules in the two training sets, very tight SCF convergence criteria and an ultrafine grid were used under optimization. Second-order derivatives were calculated analytically, and the absence of imaginary frequencies was used to confirm the minimum character of the optimized structures. Three requirements have been used in the selection of molecules for training set 1 and training set 2. First, the molecules should be experimentally well-established and preferably also have been investigated experimentally using EPR techniques. Second, the training set as a whole should be varied and represent a wide range of different ligands and coordination environments. Third, the molecules comprising training sets 1 and 2 should be computationally feasible. The last requirement naturally means that compromises between the two other requirements must be made. The scandium and zinc atoms imposed a particular challenge since they most often are found with empty or full *d* shells, respectively. Accordingly, they do not often show EPR activity, unless bounded to a radical ligand. Here, $\text{Sc}(\text{CN})_2$ and $\text{Zn}(\text{Me}_2\text{N}_2\text{C}_2\text{H}_2)\text{Cl}$ are used in training set 1. $\text{Sc}(\text{CN})_2$ is a rare d^1 EPR-active scandium system and has been identified using EPR in the gas phase. $\text{Zn}(\text{N}_2\text{C}_2\text{Me}_2)\text{Cl}$ is a model of the complex $\text{Zn}(\text{tBu}_2\text{N}_2\text{C}_2\text{H}_2)\text{Cl}$ which has been

shown to be EPR-active⁷³ due to a radical ligand. In training set 2, ZnF has been identified in the gas phase⁷⁴ and in a frozen neon matrix,⁷⁵ and the Zn hyperfine coupling tensor has been determined both experimentally⁷⁴ and theoretically.^{76,77} $\text{Sc}(\text{CO})_6$ has not been observed but is used here to represent low-valent organometallic compounds of the early d-block. TiF_3 has previously been investigated with DFT by several groups^{36,41,42,78,79} and experimentally by DeVore and Weltner⁸⁰ (EPR) and Hastie et al.⁸¹ (IR). The spin Hamilton parameters of the corresponding titanium complex in training set 2, $[\text{Ti}(\text{H}_2\text{O})_6]^{3+}$, have also been investigated experimentally,⁸² although it was not possible to resolve the hyperfine coupling to the titanium center. The structure of $[\text{Ti}(\text{H}_2\text{O})_6]^{3+}$ is known from X-ray crystallography on Ti^{3+} -doped host lattices.⁸³ The oxo complexes of vanadium and chromium in training set 1 were chosen, as they are biologically and industrially important while simultaneously being representative for the coordination chemistry of early d-block metals.⁸⁴ Structural^{85,86} (X-ray crystallography) and magnetic data,^{87,88} including EPR, exist for both compounds. Further, the EPR parameters of $\text{V}(\text{O})(\text{acac})_2$ have been investigated with DFT by Saladino and Larsen⁸⁹ and by Neese.²⁰ EPR and crystallographic data also exist for $\text{V}(\text{S}_2\text{C}_2\text{H}_2)_3$ ⁹⁰ in training set 2, whereas the chromium compound in this training set, $[\text{Cr}(\text{CO})_4]^+$, has only been identified by EPR in a solid krypton matrix.⁹¹ Likewise, MnO_3 has been matrix isolated and identified by EPR,⁹² but no other structural data exist. This molecule is known to be a difficult case and was also included in the training sets of Munzarová and Kaupp^{36,93} and by Kossmann et al.⁴¹ in their large studies of DFT functionals and their performance in prediction of hyperfine coupling parameters. It should be pointed out that we use C_{3v} symmetry for MnO_3 contrary to other studies,^{36,41,93} which use D_{3h} symmetry. With the BP86 functional, the D_{3h} geometry resulted in a structure with one imaginary frequency, corresponding to a bending motion toward C_{3v} , while the frequency analysis shows only real and positive frequencies for the C_{3v} equilibrium structure. For $[\text{Mn}(\text{N})(\text{CN})_4]^-$, which is used in test 2, experimental hyperfine couplings have also been determined.⁹⁴ The EPR parameters of $[\text{Mn}(\text{N})(\text{CN})_4]^-$ have further been investigated by DFT.^{36,42} With respect to the iron compounds in training sets 1 and 2, *trans*- $\text{Fe}(\text{en})_2\text{Cl}_2$ has not been isolated. It is used as a model for $\text{Fe}(\text{tmen})_2\text{Cl}_2$, which has been crystallographically characterized.⁹⁵ In the model, we use the same spin state ($S = 3/2$) as for the original

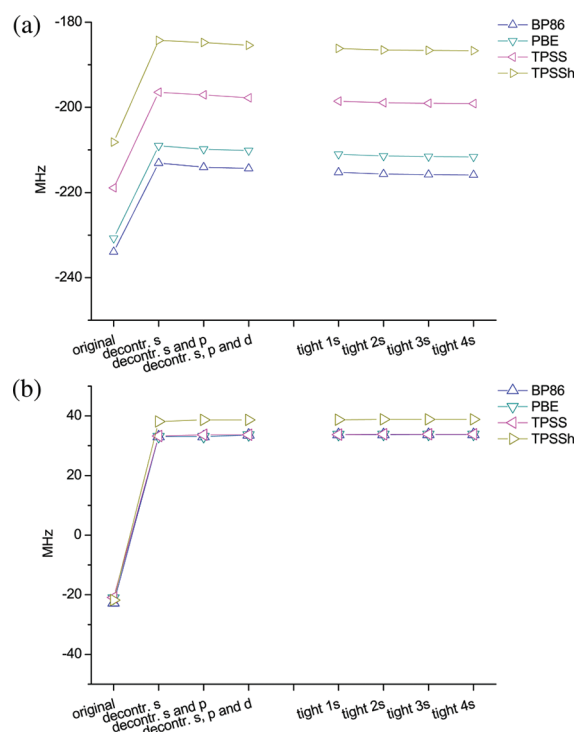


Figure 3. The effect on A_{iso} of stepwise decontraction of s-, p-, and d-type functions and further addition of four tight s-type functions for (a) TiF_3 and (b) $[\text{Cr}(\text{O})\text{Cl}_4]^-$.

complex. The structure⁹⁶ and EPR parameters⁹⁷ of $\text{Fe}(\text{NO})-(\text{Me}_2\text{dte})_2$ in training set 2 are known, and the latter have also been subjected to theoretical investigation.⁹⁸ The complexes $\text{Co}(\text{acacen})$ and $[\text{Co}(\text{Cp})(\text{CO})_2]^-$ have both been investigated using EPR^{99–101} and for $\text{Co}(\text{acacen})$ also using X-ray crystallography.¹⁰² Theoretical investigations of EPR parameters for $\text{Co}(\text{acacen})$ and $[\text{Co}(\text{Cp})(\text{CO})_2]^-$ have also been conducted.^{103–105} Turning to the nickel compounds, $[\text{Ni}(\text{mnt})_2]^-$ (training set 1) has undergone intense investigation, and both structural¹⁰⁶ and EPR data^{107–109} are known. Theoretical data on EPR parameters also exist from several sources.^{41,110,111} The corresponding complex in training set 2 is $[\text{Ni}(\text{en})_3]^{2+}$. This complex has been structurally characterized,¹¹² but no experimental hyperfine coupling parameters exist. Finally, the two copper complexes $\text{Cu}(\text{CO})_3$ and $[\text{Cu}(\text{en})_2]^{2+}$ both exist. EPR data, including Cu hyperfine coupling tensors, have been measured.^{113–115} $[\text{Cu}(\text{en})_2]^{2+}$ has also been studied by X-ray crystallography.¹¹⁶ The two compounds have also been used for DFT validation studies of EPR hyperfine coupling tensors.^{36,41,42,117}

Uncontraction and Extension of the Basis Sets. For the molecules in training set 1, the metal hyperfine coupling constants were calculated with the original and uncontracted aug-cc-pVTZ basis sets. For TiF_3 , $[\text{Cr}(\text{O})\text{Cl}_4]^-$, *trans*- $\text{Fe}(\text{en})_2\text{Cl}_2$, and $[\text{Ni}(\text{mnt})_2]^-$ molecules, the decontraction was performed in three steps, such that s-type functions were decontracted first, followed by p-type functions, and d-type functions were decontracted last. The results are shown in Figures 3 and 4. For the first coordination sphere (the atoms directly coordinated to the metal center), the same type of basis set (including the level of decontraction) as for the metal was used. Atoms not directly attached to the metal were always described with the aug-cc-pVDZ basis without any modifications. Under the addition of tight s-type functions, tight functions were added on

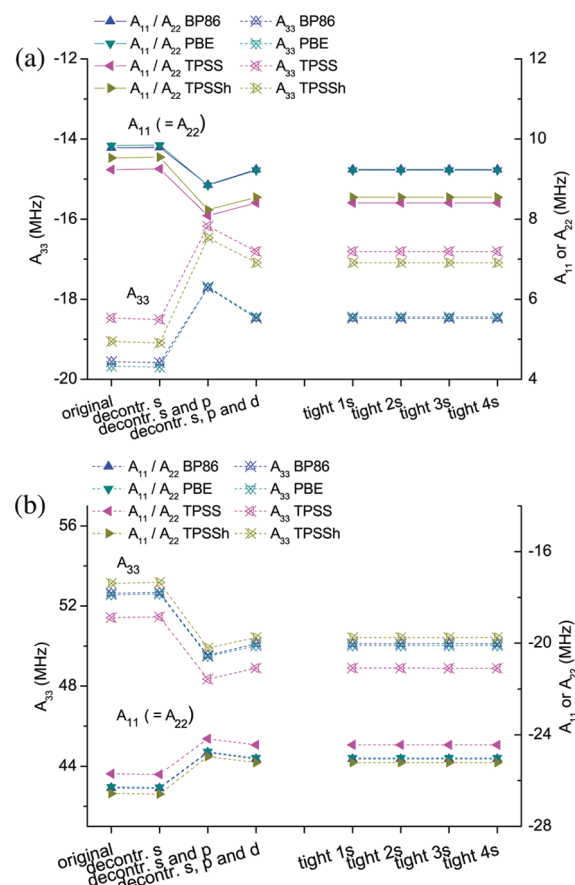


Figure 4. The effect on A_{SD} of stepwise decontraction of s-, p-, and d-type functions and further addition of four tight s-type functions for (a) TiF_3 and (b) $[\text{Cr}(\text{O})\text{Cl}_4]^-$.

both the metal and all atoms within the first coordination sphere, such that the number of added s-type functions always is the same for metal and the first coordination sphere. This was done in order to keep the basis set balanced around the metal center but allows also to investigate whether the aug-cc-pVTZ-J basis sets are adequate to describe superhyperfine couplings, i.e., couplings to ligand atoms. The result from these calculations will appear in a subsequent publication.

Basis Set Recontraction. The calculations used for the basis set reconstructions were done with the same specifications as under the decontraction. The only exception was the use of the original aug-cc-pVTZ basis for the first coordination sphere instead of a fully decontracted basis with added tight functions. We have in parallel calculations shown that modifications of the basis sets in the ligand sphere appear to have only a minor influence on the metal coupling constant.

RESULTS AND DISCUSSION

Basis Set Convergence. For the compounds TiF_3 , $[\text{Cr}(\text{O})\text{Cl}_4]^-$, *trans*- $\text{Fe}(\text{en})_2\text{Cl}_2$, and $[\text{Ni}(\text{mnt})_2]^-$ the effect on A_{iso} and A_{SD} due to stepwise decontraction of s-, p-, and d-type functions was investigated in detail. The three components in the 3×3 spin-dipolar hyperfine coupling tensor (in the diagonal representation) are here denoted A_{11} , A_{22} , and A_{33} . Due to symmetry, two of these components are equivalent in TiF_3 and $[\text{Cr}(\text{O})\text{Cl}_4]^-$ (axial symmetry), and generally

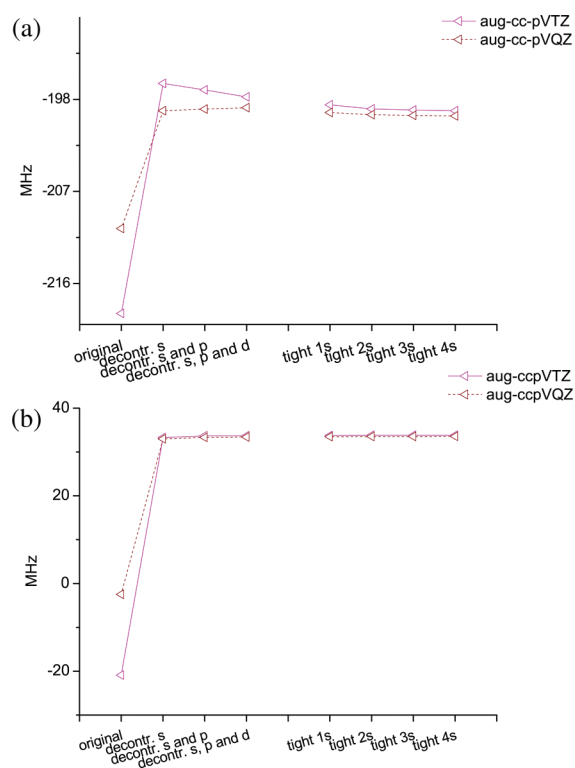


Figure 5. The effect on A_{iso} of stepwise decontraction of s-, p-, and d-type functions and further addition of four tight s-type functions using aug-cc-pVTZ and aug-cc-pVQZ basis sets for (a) TiF_3 and (b) $[Cr(O)Cl_4]^-$ (TPSS results).

the figures will be restricted to contain only these two compounds, as they are the most simple. The conclusions can be generalized to include $trans\text{-Fe(en)}_2Cl_2$ and $[Ni(mnt)_2]^-$. The convergence behavior for the isotropic and spin-dipolar coupling tensors are shown in Figures 3 and 4, respectively. For comparison, the addition of tight s-type functions is also included in these two figures. Note also that in the figure with spin dipolar tensors (Figure 4) two axes have been used, as the individual tensor components can obtain quite different values. However, the same scale is used on both axes.

The decontraction of s-type functions constitutes by far the largest contribution to A_{iso} . Decontraction of p- and d-type functions has sometimes a small effect (usually below 1 MHz). Since only s-type functions contribute directly to the spin density on the nucleus, this can be ascribed to a slightly different screening effect on the (uncontracted) s-type functions from the basis set left with contracted p- or d-type functions as compared to the basis set where these functions are uncontracted. As expected from the detailed work by Kaupp and Munzarová on spin polarization mechanisms,⁹³ decontraction of p- and d-type functions affects the dipolar term (Figure 4) and is thus generally not negligible for precise calculations. The effect on A_{iso} from decontraction of the individual s-type functions is presumably similar for the compounds $Sc(CN)_2$, $V(O)(acac)_2$, MnO_3 , $Co(acac)_3$, $Cu(CO)_3$, and $Zn(Me_2N_2C_2H_2)Cl$, for which the decontraction was performed in one step.

The addition of tight s-type functions is less important than the decontraction of s-type functions, but in order to saturate the basis set fully with respect to A_{iso} , the addition of tight functions is necessary. Although the basis sets for some of the metals in training set 1 are saturated with a lower number, four tight s-type

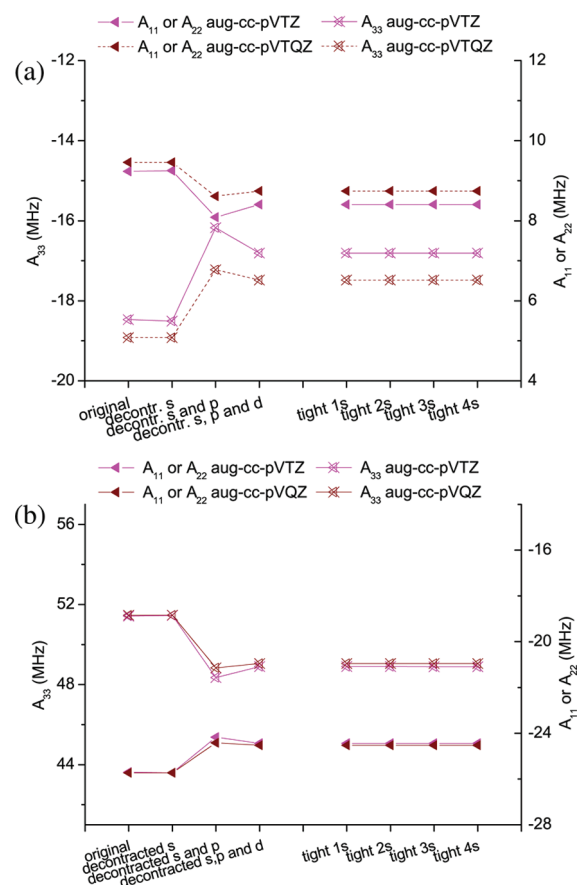


Figure 6. The effect on A_{SD} of stepwise decontraction of s-, p-, and d-type functions and further addition of four tight s-type functions using aug-cc-pVTZ and aug-cc-pVQZ basis sets for (a) TiF_3 and (b) $[Cr(O)Cl_4]^-$ (TPSS results).

functions have been added over the whole series for consistency. This is also the number of tight s-type functions used in the construction of aug-cc-pVTZ-J basis sets for p-block elements.^{51–57}

The addition of four tight p-type functions and four tight d-type functions was not necessary, but inclusion of the first tight p-type (or d-type) function sometimes shows a small effect. We have chosen to include therefore one tight p- and one tight d-type function in the final, uncontracted basis sets (see tables in the Supporting Information). These are here denoted aug-cc-pVTZ-Juc in accordance with earlier work.^{51–57}

We have also considered the quadruple- ζ basis set aug-cc-pVQZ as the underlying basis set. The result of stepwise decontraction of this basis set is shown in Figure 5 for the isotropic part and in Figure 6 for the spin-dipolar part of the hyperfine coupling tensor. Although decontraction of the s-type functions has a smaller effect on A_{iso} than with aug-cc-pVTZ basis sets, it is still by far the most important step in the decontraction. p- and d-type functions are again primarily important for the spin-dipolar part. Regarding the addition of s-type functions, three tight s-type functions are included, which again leads to basis sets similar to the main group atoms.^{51–57} The addition of tight p- and d-type functions has little or no effect on A_{iso} and A_{SD} . As was the case in the aug-cc-pVTZ-Juc basis sets, one tight p- and d-type function has been included in the final aug-cc-pVQZ-Juc basis sets. The aug-cc-pVQZ-Juc basis sets will not be considered

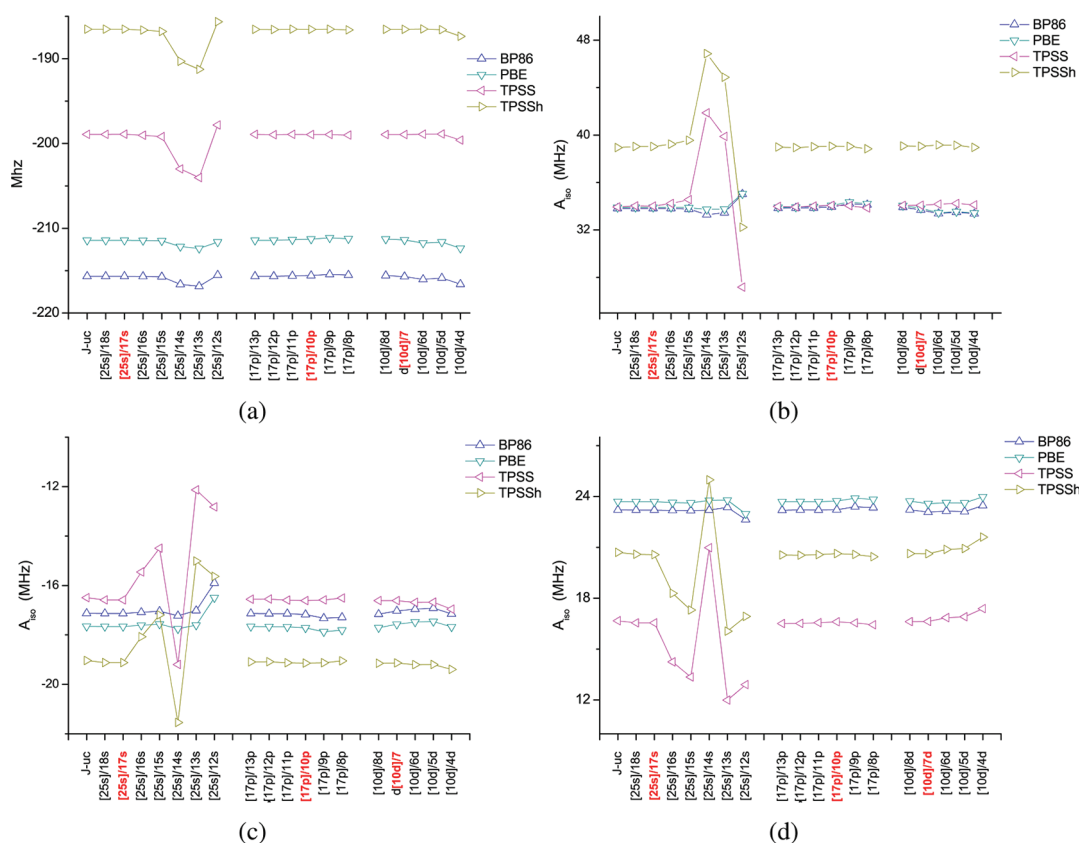


Figure 7. The effect on A_{iso} upon recontraction for (a) TiF_3 , (b) $[\text{Cr}(\text{O})\text{Cl}_4]^-$, (c) $\text{trans-Fe}(\text{en})_2\text{Cl}_2$, and (d) $[\text{Ni}(\text{mnt})_2]^-$. The red labels indicate the chosen recontraction scheme for the final basis sets.

further here, as they become too large for most purposes and the gained accuracy compared to the aug-cc-pVTZ-Juc basis sets is quite small, c.f., Figures 5 and 6.

Basis Set Recontraction. In order to reduce the size of the aug-cc-pVTZ-Juc basis set and to use it consistently with the previously developed aug-cc-pVTZ-J basis sets for lighter atoms, the uncontracted basis sets must be recontracted. As described previously,^{51–57} we use MO coefficients from a training set of molecules as contraction coefficients. In this work, the molecules in training set 1 are used. The recontraction has been done for the s-, p-, and d-type functions, separately with careful consideration of the effect on the coupling constant. This is shown for A_{iso} in Figure 7. Contrary to the decontraction study in the previous section, the investigation of how strongly the basis sets could be recontracted was performed for all molecules in training sets 1 and 2. This more extensive investigation was carried out since the effect of recontraction on A_{iso} was found to be very sensitive to both the used functional and the metal in question. Figure 7 shows a representative set of scenarios for four different molecules containing the metals Ti, Cr, Fe, and Ni. It can be seen that by recontracting the s-type functions from (25s) to [17s], using a general contraction scheme where the first 11 primitive s functions (with largest exponents) are contracted to three functions, all metals keep an accurate s-type function basis set. This contracted basis set is still converged with respect to A_{iso} , also for the metals not shown here (see the Supporting Information). More primitive s-type functions could have been included in the contracted functions for Ti and Cr (and some of the other metals,

as shown in the Supporting Information), but the chosen contraction scheme is preferred since it is consistent over the d-block.

The effect on A_{SD} is much more uniform and not nearly as dependent on functional and metal as A_{iso} (Figure 8). The focus is therefore in the following only on TiF_3 and $[\text{Cr}(\text{O})\text{Cl}_4]^-$, as these compounds have again the simplest spin dipolar tensors, while still being representative for all of the metals. A_{SD} can be described with good accuracy with a (17p) to [10p] general contraction, where the 10 primitives with highest exponents have been contracted to two functions. Finally, the d-type functions are described by a (10d) to [7d] general contraction, with the four steepest primitive d functions contracted to one function.

The method of using MO coefficients from a training set as basis set contraction coefficients has been criticized for leading to final basis sets with a bias toward the molecules within the training set.⁴⁷ Despite this concern being reasonable, it will be shown here by comparing coefficients obtained with training sets 1 and 2 that such bias is of little or no importance for the final basis sets. As an illustration, the molecular orbital coefficient of the orbitals with 1s, 2s, and 3s character are shown for TiF_3 in Figure 9.

Included in this figure are also the orbitals of 1s, 2s, and 3s character for $[\text{Ti}(\text{H}_2\text{O})_6]^{3+}$. Obviously, the compound $[\text{Ti}(\text{H}_2\text{O})_6]^{3+}$ has both different coordination geometry and also different ligands, compared to the reference compound (TiF_3). However, the titanium s-type function coefficients in TiF_3 and $[\text{Ti}(\text{H}_2\text{O})_6]^{3+}$ are very similar. This is not very surprising for the inner orbitals 1s and 2s, but even for the 3s orbital, which lies just below the valence orbitals, the coefficients are still almost identical. Figure 10 compares the TiF_3 and $[\text{Ti}(\text{H}_2\text{O})_6]^{3+}$ MO coefficients for the

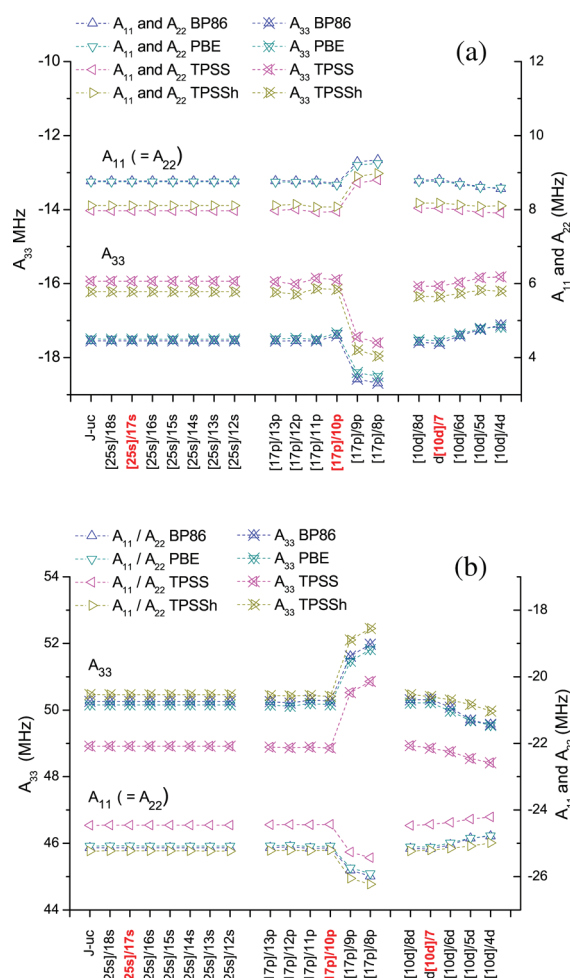


Figure 8. The effect on A_{SD} upon recontraction for (a) TiF_3 and (b) $[\text{Cr}(\text{O})\text{Cl}_4]^-$. The red labels indicate the chosen recontraction scheme for the final basis sets.

primitive Ti p_z orbitals in the MOs of 2p and 3p character on titanium. The same conclusion as for the s-type functions is reached: For the 2p and even for the 3p orbital, the coefficients are almost identical and thus apparently rather independent of the compound. Closer analysis shows, however, that differences in MO coefficients are larger for the more diffuse orbitals, while primitives with large exponents always have almost identical coefficients. Only the d orbitals show slightly different MO coefficients for the primitives (see Figure 11). But the d orbitals are in general more difficult, as they comprise the valence electrons. Accordingly, the d shell is usually partly filled, and it is not always possible to use the same d orbital in the reference compound (from training set 1) as in the corresponding compound in training set 2. Therefore, only the first four primitives are included in the contraction, as the MO coefficients for these are almost identical.

We have carefully tested all other molecules in training sets 1 and 2 in this manner and reach the same conclusions as for TiF_3 and $[\text{Ti}(\text{H}_2\text{O})]^{3+}$. With the great span of metals and different ligand spheres in these two training sets, we thus conclude that the method of using MO coefficients as recontraction coefficients leads to basis sets with little or no bias. As a final comment on this matter, we did also perform a calculation with the Mn^{2+} ion. This calculations showed the coefficients to vary little between mole-

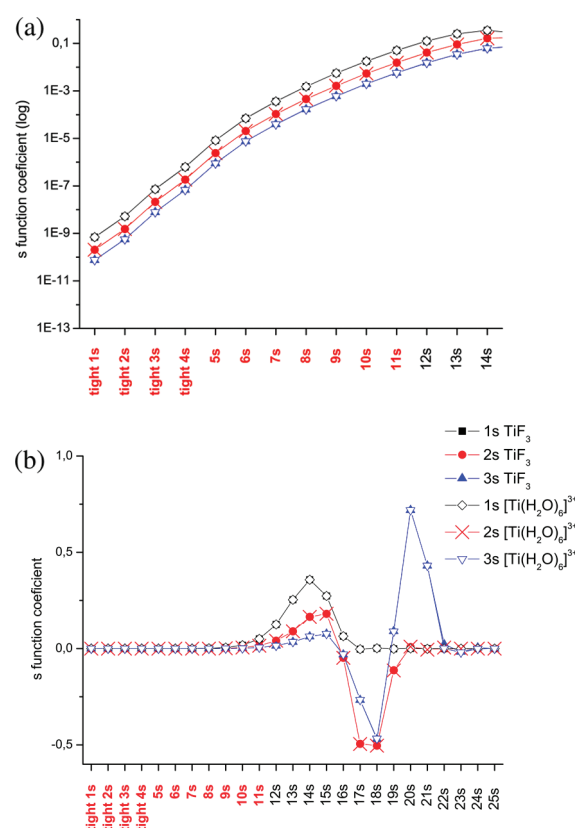


Figure 9. (a) The first 14 MO coefficients for Ti s-type primitives in the orbitals with 1s, 2s, and 3s character for Ti (logarithmic scale). (b) The full range of all 25 s-type primitives where the first four are the added tight functions and the remaining 21 from the original aug-cc-pVTZ basis set (TPSS results). The primitive functions with red labels are the primitives used in the reconstructions.

cules and atoms, but to establish this relationship more firmly, more extensive calculations using several ions or neutral atoms would be needed.

Dependence on Exchange-Correlation Functional. *Contraction Coefficients.* For the compounds TiF_3 , $[\text{Cr}(\text{O})\text{Cl}_4]^-$, $\text{trans-Fe}(\text{en})_2\text{Cl}_2$, and $[\text{Ni}(\text{mnt})_2]^-$, the effect of using different functionals on the values of the contraction coefficients was investigated in some detail. In line with other studies on main group atoms,^{47,57} this turned out to be of little importance. As an example, the MO coefficients for the titanium p- and d-type primitives in orbitals of 3p and 3d character are shown in Figure 12. The same pattern as in Figure 12 is seen for the other three compounds.

Hyperfine Coupling Constants. It is noted by comparing Figure 3a and b that the metal isotropic hyperfine coupling tensor is very sensitive to the used functional, although this dependence again depends on the metal in question. Thus, a much wider span in the final hyperfine coupling constants arises from the four applied functionals for TiF_3 , compared to $[\text{Cr}(\text{O})\text{Cl}_4]^-$. As can be seen from the tables collected in the Supporting Information, the span in the final A_{iso} values for the four different functionals is very different across the series of 3d metals. However, the convergence behavior in the basis sets is always completely similar for all of the functionals used. This is also the case for the dipolar couplings, although the final values in A_{SD} depend much less critically on the applied functional (here, the spans are within 2 MHz).

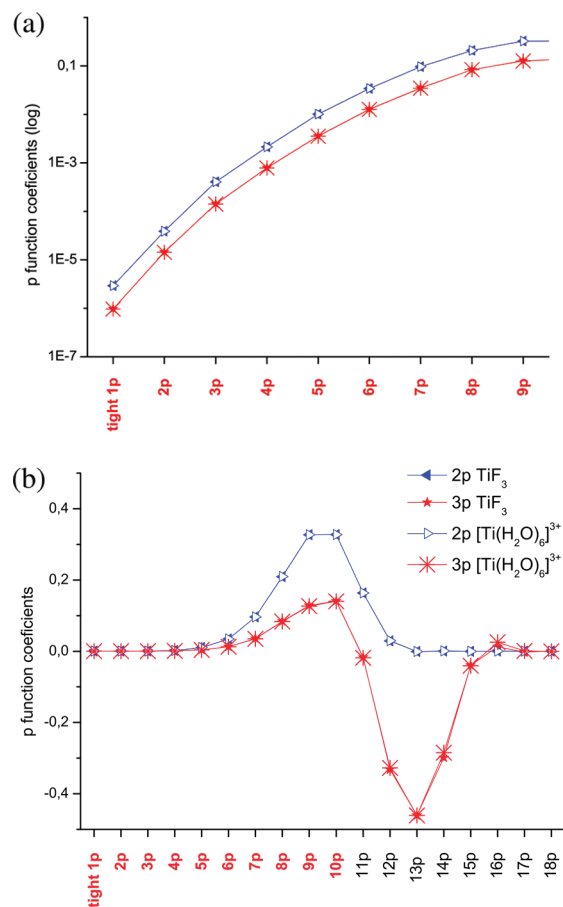


Figure 10. (a) The first nine MO coefficients for titanium p-type primitives in the orbitals of titanium 2p_z and 3p_z character (logarithmic scale). (b) The full range of all 17 p-type primitives where the first is the added tight function and the remaining 16 are from the original aug-cc-pVTZ basis set (TPSS results). The primitive functions with red labels are the primitives used in the reconstructions.

In the case of MnO₃, inclusion of exact exchange occasionally leads to complete deterioration of the results, and for this special case, hybrid functionals are not recommended. The same conclusion was reached by Kaupp and Munzarová⁹³ even though they used a different equilibrium geometry (*D*_{3h}). The equilibrium geometry itself of this molecule is also very dependent on the used functional; where the hybrid functional B3LYP leads to an equilibrium structure of *D*_{3h} symmetry, the BP86 functional used here leads instead to a *C*_{3v} equilibrium geometry.

The difference in the effect of recontraction upon both *A*_{iso} and *A*_{SD} is also quite pronounced. Here, *meta*-GGA functionals are found to be most sensitive to the level of recontraction, and a much more conservative choice of recontraction scheme must be chosen when such functionals are used. Detailed investigation of the underlying mechanisms are currently being undertaken.

COMPARISON WITH EXPERIMENT

A comparison of measured hyperfine coupling constants with results of calculations at equilibrium geometries is not trivial, as both environmental effects from solvation and ro-vibrational contributions can have substantial effects on the calculated values. Furthermore, for transition metals also relativistic effects can be

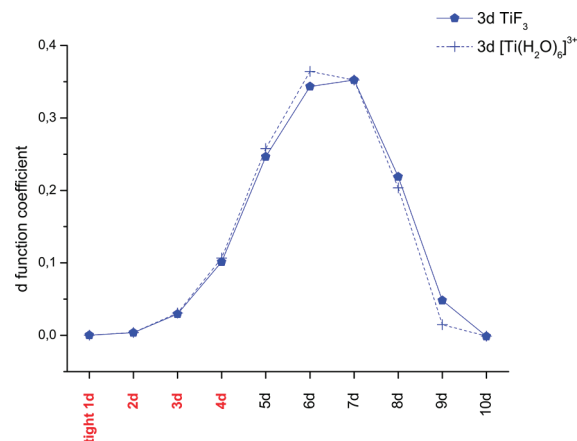


Figure 11. The 10 MO coefficients for titanium d-type primitives in the orbitals of titanium 3d_{z²} character. The first function is the added tight function, and the remaining nine are from the original aug-cc-pVTZ basis set (TPSS results). The primitive functions with red labels are the primitives used in the reconstructions.

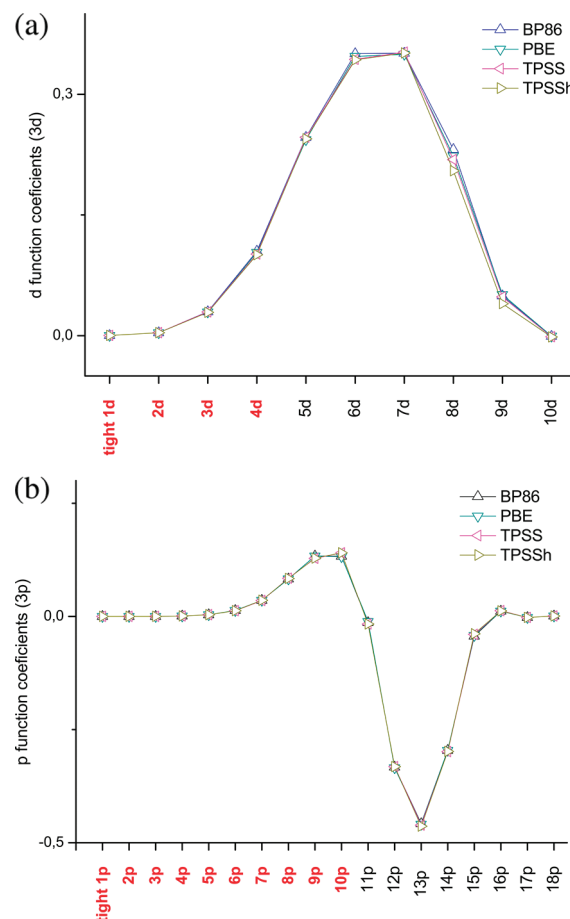


Figure 12. MO coefficients for Ti p- and d-type primitives in the orbitals of 3p (a) and 3d (b) character for TiF₃. The primitive functions with red labels are the primitives used in the reconstructions.

important. Nevertheless, some of the compounds from training set 1, where the hyperfine coupling has been resolved from the experimental EPR spectrum, are here compared to the calculated

Table 1. Calculated versus Experimental Values for Hyperfine Coupling Tensors (TPSS Results)

molecule	basis	A_{11}^{SD}	A_{22}^{SD}	A_{33}^{SD}	A_{iso}
TiF ₃	aug-cc-pVTZ	9.23	9.23	−18.47	−218.93
	aug-cc-pCVTZ	8.61	8.61	−17.21	−199.13
	aug-cc-pVTZ-J	8.03	8.03	−16.07	−198.95
exptl. ⁸⁰		6.60	6.60	−12.40	−184.8
V(O)(acac) ₂	aug-cc-pVTZ	94.49	108.24	−202.73	26.82
	aug-cc-pCVTZ	104.13	91.13	−195.3	−144.87
	aug-cc-pVTZ-J	104.21	92.03	−196.24	−219.26
exptl. ⁸⁷		116	112	−228	−307
MnO ₃	aug-cc-pVTZ	−18.87	−18.87	37.73	−124.16
	aug-cc-pCVTZ	−90.59	−90.58	181.17	1818.62
	aug-cc-pVTZ-J	−92.83	−92.83	185.66	1754.11
exptl. ⁹²		−80.00	−80.00	160.00	1612.00
Cu(CO) ₃	aug-cc-pVTZ	−57.21	−57.21	114.43	−18.62
	aug-cc-pCVTZ	−47.91	−47.91	117.50	−9.30
	aug-cc-pVTZ-J	−59.25	−59.25	118.50	2.67
exptl. ¹¹³		−81.17	−81.17	162.33	71.17

hyperfine couplings in Table 1 (see also Supporting Information). The original aug-cc-pVTZ and the core-correlation basis set aug-cc-pCVTZ are also included for comparison. Although the aug-cc-pCVTZ basis sets lead to some improvement over the original aug-cc-pVTZ basis sets, the results are still quite far from the converged aug-cc-pVTZ-J basis set results (all results in Table 1 are obtained with the TPSS functional). For most of the shown examples, reasonable qualitative agreement is obtained between experimental hyperfine coupling tensors and the aug-cc-pVTZ-J basis set results. Nevertheless, it is clear that more work is needed to obtain quantitative agreement between theory and experiment.

The compound MnO₃ is of some interest, since the functional used for geometry optimization (BP86) yielded a C_{3v} structure, rather than the experimentally observed D_{3h} structure, while the B3LYP functional leads to the D_{3h} structure. However, the experimental structure is deduced from the size of the ⁵⁵Mn hyperfine coupling alone, and the studies presented here show that couplings of similar magnitude are calculated from a C_{3v} equilibrium structure. A detailed study of the MnO₃ equilibrium structure is beyond the scope of this work, but these observations definitely call for further investigations.

CONCLUSIONS

The aug-cc-pVTZ-J series of basis sets has been extended to the 3d metals Sc–Zn. First, the convergence of the Fermi-contact and spin-dipolar terms (A_{iso} and A_{SD}) was investigated with respect to decontracting the s-, p-, and d-type functions in the original aug-cc-pVTZ basis sets and then further with respect to the addition of tight s-, p-, and d-type functions. As discovered for the main group elements, the original aug-cc-pVTZ basis sets are too contracted in the s shells to describe core properties.¹¹⁸ The training set used in the generation of the basis sets consisted mainly of experimentally well-known compounds, which often also have been studied using EPR techniques.

In order to prevent bias toward a particular exchange-correlation functional, we have employed four different functionals. Although there were found to be quite substantial differences in the final predicted values of especially A_{iso} , the convergence of the results with respect to decontraction of the basis sets and the

addition of tight functions was generally not dependent on the employed functional. A modification of aug-cc-pVTZ (uncontracted) with four added tight s-type functions, one tight p-, and one tight d-type function was found to give a hyperfine coupling tensor which was saturated with respect to the basis set. This basis set is denoted aug-cc-pVTZ-Juc, which comprises a 25s17p10d3f2g set of functions. These uncontracted basis sets have been recontracted to the final aug-cc-pVTZ-J basis sets according to (25s17p10d3f2g)/[17s10p7d3f2g] and using a general contraction scheme. MO coefficients from the molecules in a training set (training set 1) were used as contraction coefficients. By careful comparison with a second training set (training set 2), it could be shown that a possible bias toward the molecules in training set 1 largely was avoided. Furthermore, the obtained coefficients have been shown to be insensitive to the functional used. Future work will be directed to benchmark the final aug-cc-pVTZ-J basis sets against a larger compilation of systems with experimentally known hyperfine coupling constants employing a larger set of functionals and also high-level *ab initio* methods.

ASSOCIATED CONTENT

S Supporting Information. Detailed tables of the calculated hyperfine coupling constants (experimental data is included when available) at different contraction levels. With the exception of Figures 5 and 6, all figures have been constructed from these tables. The data from Figures 5 and 6 can be obtained from E.D.H. (edh@ifk.sdu.dk). This material is available free of charge via the Internet at <http://pubs.acs.org>.

AUTHOR INFORMATION

Corresponding Author

*E-mail: sauer@kiku.dk.

Notes

The authors declare no competing financial interest.

ACKNOWLEDGMENT

This work has been supported by the Danish Center for Scientific Computing and the Danish Natural Science Research Council/Danish Councils for Independent Research. J.K. thanks the Lundbeck Foundation and S.P.A.S thanks the Carlsberg foundation for financial support.

REFERENCES

- (1) Kaupp, M.; Bühl, M.; Malkin, V. G. *Calculation of NMR and EPR Parameters. Theory and Applications*; Wiley: New York, 2004.
- (2) Bleaney, B.; Abragam, A. *Electron Paramagnetic Resonance of Transition Metal Ions*; Oxford University Press: Oxford, U. K., 1970.
- (3) Tuttle, T. R., Jr.; Ward, R. L.; Weissman, S. I. *J. Chem. Phys.* **1956**, 25, 189–189.
- (4) Katz, T. J.; Strauss, H. L. *J. Chem. Phys.* **1960**, 32, 1873–1875.
- (5) Fessenden, R. W.; Schuler, R. H. *J. Chem. Phys.* **1963**, 39, 2147–2195.
- (6) Schäfer, K. O.; Bittl, R.; Lendzian, F.; Barynin, V.; Weyhermüller, K.; Wieghardt, T.; Lubitz, W. *J. Phys. Chem. B* **2003**, 107, 1242–1250.
- (7) Veselov, A.; Sun, H.; Sienkiewicz, A.; Taylor, H.; Burger, R. M.; Scholes, C. P. *J. Am. Chem. Soc.* **1995**, 117, 7508–7512.
- (8) Veselov, A.; Burger, R. M.; Scholes, C. P. *J. Am. Chem. Soc.* **1998**, 120, 1030–1033.
- (9) Pryce, M. L. H. *Phys. Rev.* **1950**, 80, 1107–1108.

- (10) Bleaney, B.; Ingram, D. J. E. *Proc. Phys. Soc. A* **1950**, *63*, 409–411.
- (11) Abragam, A.; Pryce, M. L. H. *Proc. R. Soc. London, Ser. A* **1951**, *205*, 135–153.
- (12) Abragam, A.; Pryce, M. L. H. *Proc. R. Soc. London, Ser. A* **1951**, *206*, 173–191.
- (13) Abragam, A.; Horowitz, J.; Pryce, M. L. H.; Morton, K. W. *Proc. R. Soc. London, Ser. A* **1955**, *230*, 169–187.
- (14) Davydov, R.; Kappl, R.; Hüttermann, J.; Peterson, J. A. *FEBS Lett.* **1991**, *295*, 113–115.
- (15) Davydov, R.; Makris, T. M.; Kofman, V.; Werst, D. E.; Sligar, S. G.; Hoffman, B. M. *J. Am. Chem. Soc.* **2001**, *123*, 1403–1415.
- (16) Davydov, R.; Satterlee, J. D.; Fujii, H.; Sauer-Masarwa, A.; Busch, D. H.; Hoffman, B. M. *J. Am. Chem. Soc.* **2003**, *125*, 16340–16346.
- (17) Davydov, R.; Perera, R.; Jin, S.; Yang, T.; Bryson, T. A.; Sono, M.; Dawson, J. D.; Hoffman, B. M. *J. Am. Chem. Soc.* **2005**, *127*, 1403–1413.
- (18) Mukhopadhyay, S.; Mandal, S. K.; Bhaduri, S. S.; Armstrong, W. H. *Chem. Rev.* **2004**, *104*, 3981–4026.
- (19) Sauer, S. P. A. *Molecular Electromagnetism: A Computational Chemistry Approach*; Oxford University Press: Oxford, U. K., 2011.
- (20) Neese, F. *J. Chem. Phys.* **2003**, *118*, 3939–2948.
- (21) Watson, R. E.; Freeman, A. J. *Phys. Rev.* **1961**, *123*, 2027–2047.
- (22) Engels, B.; Peyerimhoff, S. D.; Karna, S. P.; Grein, F. *Chem. Phys. Lett.* **1988**, *152*, 397–401.
- (23) Engels, B.; Peyerimhoff, S. D. *J. Phys. B: At. Mol. Opt. Phys.* **1988**, *88*, 3459–3471.
- (24) Feller, D.; Davidson, E. R. *J. Chem. Phys.* **1988**, *88*, 7580–7587.
- (25) Bauschlicher, C. W., Jr.; Langhoff, S. R.; Partridge, H.; Chong, D. P. *J. Chem. Phys.* **1988**, *89*, 2985–2992.
- (26) Funken, K.; Engels, B.; Peyerimhoff, S. D.; F. Grein, F. *Chem. Phys. Lett.* **1990**, *172*, 180–186.
- (27) Chipman, D. M.; Carmicheal, I.; Feller, D. *J. Phys. Chem.* **1991**, *95*, 4702–4708.
- (28) Engels, B. *Chem. Phys. Lett.* **1991**, *179*, 398–404.
- (29) Engels, B. *Theor. Chim. Acta* **1993**, *86*, 429–437.
- (30) Engels, B. *J. Chem. Phys.* **1994**, *100*, 1380–1386.
- (31) Perera, S. A.; Watt, J. D.; Bartlett, R. J. *J. Chem. Phys.* **1994**, *100*, 1425–2434.
- (32) Kong, J.; Boyd, R. J.; Erikson, L. A. *J. Chem. Phys.* **1995**, *102*, 3674–3678.
- (33) Engels, B. *Acta Chem. Scand.* **1997**, *51*, 199–210.
- (34) Chipman, D. M. *Phys. Rev.* **1989**, *39*, 475.
- (35) Knight, L. B., Jr.; Babb, R.; Ray, M.; Banisaukas, T. J., III; Russon, L.; Dailey, S.; Davidson, E. R. *J. Chem. Phys.* **1996**, *105*, 10237–10250.
- (36) Munzarová, M.; Kaupp, M. *J. Phys. Chem. A* **1999**, *103*, 9966–9983.
- (37) Ishii, N.; Shimizu, T. *Chem. Phys. Lett.* **1994**, *225*, 462–466.
- (38) Ishii, N.; Shimizu, T. *Chem. Phys. Lett.* **1995**, *235*, 614–616.
- (39) Barone, V. *Theor. Chem. Acc.* **1995**, *91*, 113–128.
- (40) Batra, R.; Giese, B.; Spichty, M.; Gescheidt, G.; Houk, K. N. *J. Phys. Chem.* **1996**, *100*, 18371–18379.
- (41) Kossmann, S.; Kirchner, B.; Neese, F. *Mol. Phys.* **2007**, *105*, 2049.
- (42) Abuznikov, A. V.; Kaupp, M.; Malkin, V. G.; Reviakine, R.; Malkina, O. L. *Phys. Chem. Chem. Phys.* **2002**, *4*, 5467–5474.
- (43) Chipman, D. M. *Theor. Chim. Acta* **1989**, *76*, 73–84.
- (44) Chipman, D. M. *J. Chem. Phys.* **1989**, *91*, 5455–5465.
- (45) Chipman, D. M. *Theor. Chim. Acta* **1992**, *82*, 93–115.
- (46) Barone, V. In *Recent Advances in Density Functional Methods Part I*; Chong, D. P., Ed.; World Scientific: Singapore, 1996.
- (47) Jensen, F. *J. Chem. Theory Comput.* **2006**, *2*, 1360–1369.
- (48) Barone, V.; Cimino, P.; Stendardo, E. *J. Chem. Theory Comput.* **2008**, *4*, 751–764.
- (49) Kjær, H.; Sauer, S. P. A. *J. Chem. Theory Comput.* **2011**, Online: <http://dx.doi.org/10.1021/ct200546q>.
- (50) Neese, F. *Inorg. Chim. Acta* **2002**, *337*, 181–192.
- (51) Enevoldsen, T.; Oddershede, J.; Sauer, S. P. A. *Theor. Chem. Acc.* **1998**, *100*, 275–284.
- (52) Sauer, S. P. A.; Raynes, W. T. *J. Chem. Phys.* **2000**, *113*, 3121–3129.
- (53) Sauer, S. P. A.; Raynes, W. T.; Nicholls, R. A. *J. Chem. Phys.* **2001**, *115*, 5994–6006.
- (54) Provasi, P. F.; Aucar, G. A.; Sauer, S. P. A. *J. Chem. Phys.* **2001**, *115*, 1324–1334.
- (55) Barone, V.; Provasi, P. F.; Peralta, J. E.; Snyder, J. P.; Sauer, S. P. A.; Contreras, R. H. *J. Phys. Chem. A* **2003**, *107*, 4748–4754.
- (56) Rusakov, Y. Y.; Krivdin, L. B.; Sauer, S. P. A.; Levanova, E. P.; Levkovskaya, G. G. *Magn. Reson. Chem.* **2010**, *48*, 633–637.
- (57) Provasi, P. F.; Sauer, S. P. A. *J. Chem. Phys.* **2010**, *133*, 054308.
- (58) Neese, F. ORCA - An ab initio, DFT and semiempirical Program package, Version 2.7. University of Bonn, 2009.
- (59) Erikson, L. A.; Wang, J.; Boyd, R. J. *Chem. Phys. Lett.* **1993**, *211*, 88–93.
- (60) Erikson, L. A.; Wang, J.; Boyd, R. J.; Lunell, S. J. *Phys. Chem.* **1994**, *98*, 792–799.
- (61) Erikson, L. A.; Malkina, O. L.; Malkin, V. G.; Salahub, D. R. *J. Chem. Phys.* **1994**, *100*, S066–S075.
- (62) Becke, A. D. *J. Chem. Phys.* **1993**, *98*, 5648–5652.
- (63) Perdew, J. P. *Phys. Rev. B* **1986**, *33*, 8822–8824.
- (64) Perdew, J. P.; Burke, K.; Wang, Y. *Phys. Rev. Lett.* **1996**, *77*, 3865–3868. Erratum: **1997**, *78*, 1396.
- (65) Tao, J.; Perdew, J. P.; Staroverov, G. E. *Phys. Rev. Lett.* **2003**, *91*, 146401.
- (66) Dunning, T. H., Jr. *J. Chem. Phys.* **1989**, *90*, 1007–1023.
- (67) Kendall, R. A.; Dunning, T. H.; Harrison, R. J. *J. Chem. Phys.* **1992**, *96*, 6796–6806.
- (68) Woon, D. E.; Dunning, T. H., Jr. *J. Chem. Phys.* **1993**, *98*, 1358–1371.
- (69) Balabanov, N. B.; Peterson, K. A. *J. Chem. Phys.* **2005**, *123*, 64107.
- (70) Frisch, M. J.; Trucks, G. W.; Schlegel, H. B.; Scuseria, G. E.; Robb, M. A.; Cheeseman, J. R.; Scalmani, G.; Barone, V.; Mennucci, B.; Petersson, G. A.; Nakatsuji, H.; Caricato, M.; Li, X.; Hratchian, H. P.; Izmaylov, A. F.; Bloino, J.; Zheng, G.; Sonnenberg, J. L.; Hada, M.; Ehara, M.; Toyota, K.; Fukuda, R.; Hasegawa, J.; Ishida, M.; Nakajima, T.; Honda, Y.; Kitao, O.; Nakai, H.; Vreven, T.; Montgomery, J. A., Jr.; Peralta, J. E.; Ogliaro, F.; Bearpark, M.; Heyd, J. J.; Brothers, E.; Kudin, K. N.; Staroverov, V. N.; Kobayashi, R.; Normand, J.; Raghavachari, K.; Rendell, A.; Burant, J. C.; Iyengar, S. S.; Tomasi, J.; Cossi, M.; Rega, N.; Millam, N. J.; Klene, M.; Knox, J. E.; Cross, J. B.; Bakken, V.; Adamo, C.; Jaramillo, J.; Gomperts, R.; Stratmann, R. E.; Yazyev, O.; Austin, A. J.; Cammi, R.; Pomelli, C.; Ochterski, J. W.; Martin, R. L.; Morokuma, K.; Zakrzewski, V. G.; Voth, G. A.; Salvador, P.; Dannenberg, J. J.; Dapprich, S.; Daniels, A. D.; Farkas, Ö.; Foresman, J. B.; Ortiz, J. V.; Cioslowski, J.; Fox, D. J. *Gaussian 09*, Revision A.1.; Gaussian Inc.: Wallingford, CT, 2009.
- (71) Schäfer, A.; Horn, H.; Ahlrichs, R. *J. Chem. Phys.* **1992**, *97*, 2571–2577.
- (72) Schäfer, A.; Huber, C.; Ahlrichs, R. *J. Chem. Phys.* **1994**, *100*, 5829–5835.
- (73) Clopach, P.; von Zelewsky, A. *Helv. Chim. Acta* **1972**, *55*, 52–67.
- (74) Flory, M. A.; McLamarrah, S. K.; Ziurys, L. M. *J. Chem. Phys.* **2006**, *125*, 194304.
- (75) Knight, J. B., Jr.; Mouchet, A.; Beaudry, W. T.; Duncan, M. *J. Magn. Reson.* **1978**, *32*, 383–390.
- (76) Belanzoni, P.; van Lenthe, E.; Baerends, E. J. *J. Chem. Phys.* **2001**, *114*, 4421–4433.
- (77) Malkin, I.; Malkina, O. L.; Malkin, V. G.; Kaupp, M. *Chem. Phys. Lett.* **2004**, *396*, 268–276.
- (78) Belanzoni, P.; Baerends, E. J.; van Asselt, S.; Langewen, P. B. *J. Phys. Chem.* **1995**, *99*, 13094–13102.
- (79) Belanzoni, P.; Baerends, E. J.; Gribnau, M. *J. Phys. Chem. A* **1999**, *103*, 3732–3744.
- (80) DeVore, T. C.; Weltner, W., Jr. *J. Am. Chem. Soc.* **1977**, *99*, 4700–4703.
- (81) Hastie, J. W.; Hauge, R. H.; Margrave, J. L. *J. Chem. Phys.* **1969**, *51*, 2648–2656.

- (82) Carver, G.; Bendix, J.; Tregenna-Piggot, P. L. W. *Chem. Phys.* **2002**, *282*, 245–263.
- (83) Sygusch, J. *Acta Crystallogr., Sect. B* **1974**, *30*, 662–665.
- (84) Nugent, W. A.; Mayer, J. M. *Metal-Ligand Multiple Bonds: The Chemistry of Transition Metal Complexes Containing Oxo, Nitrido, Imido, Alkylidene, or Alkylidyne Ligands*; Wiley: New York, 1988.
- (85) Dodge, R. P.; Templeton, D. H. *J. Chem. Phys.* **1969**, *35*, 55–67.
- (86) Gahan, B.; Garner, C. D.; Hill, L. H.; Mabbs, F. E.; Hargave, K. D.; McPhail, A. T. *J. Chem. Soc., Dalton Trans.* **1977**, 1726–1729.
- (87) Campbell, R. F.; Freed, K. F. *J. Phys. Chem.* **1980**, *84*, 2668–2680.
- (88) Garner, C. D.; Hillier, I. H.; Mabbs, F. E.; Taylor, C.; Guest, M. F. *J. Chem. Soc., Dalton Trans.* **1976**, 2258.
- (89) Saladino, A. C.; Larsen, S. C. *J. Phys. Chem. A* **2003**, *107*, 1872–1878.
- (90) Kondo, M.; Minakoshi, S.; Iwata, K.; Shimizu, T.; Matsuzaka, H.; Kamigata, N.; Kitagawa, S. *Chem. Lett.* **1996**, 489–490.
- (91) Fairhurst, S. A.; Morton, J. R.; Preston, K. F. *Chem. Phys. Lett.* **1984**, *104*, 112–114.
- (92) Ferrante, R. F.; Wilkerson, J. L.; Graham, W. R. M.; Weltner, W., Jr. *J. Chem. Phys.* **1977**, *67*, S904–S913.
- (93) Munzarová, M.; Kaupp, M. *J. Am. Chem. Soc.* **2000**, *122*, 11900–11913.
- (94) Bendix, J.; Meyer, K.; Weyhermüller, T.; Bill, E.; Metzler-Nolte, N.; Wieghardt, K. *Inorg. Chem.* **1998**, *37*, 1767–1775.
- (95) Davies, S. C.; Hughes, D. L.; Leigh, J. R.; Sanders, G. J.; de Souza, J. S. *J. Chem. Soc., Dalton Trans.* **1997**, 1981–1988.
- (96) Davies, G. R.; Jarvis, J. A. J.; Kilbourn, B. T.; Mais, R. H. B.; Owston, P. G. *J. Chem. Soc. A* **1970**, 1275–1283.
- (97) Feltham, R. D.; Crain, H. *Inorg. Chem. Acta* **1980**, *40*, 37–40.
- (98) Dethlefsen, J. W.; Hedegård, E. D.; Rimmer, R. D.; Ford, P. C.; Døssing, A. *Inorg. Chem.* **2009**, *48*, 231–238.
- (99) Rudin, M.; Schweiger, A.; Berchten, N.; Günthard, H. H. *Mol. Phys.* **1980**, *41*, 1317.
- (100) Rudin, M.; Jörin, E.; Schweiger, A.; Günthard, H. H. *Chem. Phys. Lett.* **1979**, *67*, 374–376.
- (101) Symons, M. C. R.; Bratt, S. W. *J. Chem. Soc., Dalton Trans.* **1979**, 1739–1743.
- (102) Cariati, F.; Morazzoni, F.; Busetto, C.; Del Piero, G.; Zazzetta, A. *J. Chem. Soc., Dalton Trans.* **1976**, 342–347.
- (103) Atanasov, M.; Baerends, E. J.; Baettig, P.; Bruyndonckx, R.; Daul, C.; Rauzy, C.; Zbiri, Z. *Chem. Phys. Lett.* **2004**, *399*, 433.
- (104) Zbiri, M. *Inorg. Chim. Acta* **2006**, *359*, 3865–3870.
- (105) Braden, D. A.; Tyler, D. R. *J. Am. Chem. Soc.* **1998**, *120*, 942–947.
- (106) Kobayashi, A.; Sasaki, Y. *Bull. Chem. Soc. Jpn.* **1977**, *50*, 2650–2656.
- (107) Maki, A. H.; Edelstein, N.; Davison, A.; Holm, R. H. *J. Am. Chem. Soc.* **1964**, *86*, 4580–4587.
- (108) Schmitt, R. D.; Holm, R. H. *J. Am. Chem. Soc.* **1968**, *90*, 2288–2292.
- (109) Huyett, J. E.; Choudhury, S. B.; Eichhorn, D. M.; Bryngelson, P. A.; Maroney, M. J.; Hoffman, B. M. *Inorg. Chem.* **1998**, *37*, 1361–1367.
- (110) Stein, M.; van Lenthe, E.; Baerends, E. J.; Lubitz, W. *J. Phys. Chem. A* **2001**, *105*, 416–425.
- (111) Stadler, C.; de Lacey, A. L.; Hernández, B.; M., F. V.; Conesa, J. C. *Inorg. Chem.* **2002**, *41*, 4417–4423.
- (112) Swink, L. N.; Atoji, M. *Acta Crystallogr.* **1960**, *13*, 639–643.
- (113) Kasai, P. H.; Jones, P. M. *J. Am. Chem. Soc.* **1985**, *107*, 813–818.
- (114) Huber, H.; Kündig, E. P.; Moskovits, M.; Ozin, G. A. *J. Am. Chem. Soc.* **1975**, *97*, 2097–2106.
- (115) Sastry, B. A.; Asadullah, S. M.; Ponticelli, P.; Massacei, M. *Spectrochim. Acta* **1979**, *35A*, 817–821.
- (116) Maxcy, K. R.; Turnbull, M. M. *Acta Crystallogr., Sect. C* **1999**, *C55*, 1986–1988.
- (117) Neese, F. *J. Phys. Chem. A* **2001**, *105*, 4290–4299.
- (118) Gauld, J. W.; Erikson, L. A.; Radom, L. *J. Chem. Phys.* **1997**, *101*, 1352–1359.